Synthesis of Polymer Brushes Composed of Poly(phenylacetylene) Main Chain and Either Polystyrene or Poly(methyl methacrylate) Side Chains

Wei Zhang,[†] Masashi Shiotsuki,[†] Toshio Masuda,*[,†] Jiro Kumaki,[‡] and Eiji Yashima[‡,§]

Department of Polymer Chemistry, Graduate School of Engineering, Kyoto University, Katsura Campus, Kyoto 615-8510, Japan, Yashima Super-structured Helix Project, Exploratory Research for Advanced Technology (ERATO), Japan Science and Technology Agency (JST), 101 Creation Core Nagoya, Shimoshidami, Moriyama-ku, Nagoya 463-0003, Japan, and Department of Molecular Design and Engineering, Graduate School of Engineering, Nagoya University, Chikusa-ku, Nagoya 464-8603, Japan

Received August 24, 2006; Revised Manuscript Received November 15, 2006

ABSTRACT: Novel cylindrical polymer brushes consisting of a highly cis-transoidal poly(phenylacetylene) main chain and either polystyrene (PS) or poly(methyl methacrylate) (PMMA) side chains were synthesized by the macromonomer method. Two phenylacetylene-terminated macromonomers, namely, M−PS (M_n = 1830) and M−PMMA (M_n = 1860), were prepared by atom transfer radical polymerization (ATRP) of styrene and methyl methacrylate, respectively, using acetylene-functionalized initiators. M−PS and M−PMMA were polymerized successfully with the $[(nbd)RhCl]_2/Et_3N$ (2,5-norbornadiene) catalyst [Rh-**1**] to give high molecular weight polymer brushes, poly(M−PS) (e.g., M_w 1660 × 10^3) and poly(M−PMMA) (e.g., M_w 1480 × 10^3), respectively, according to GPC−RALLS. Further, well-defined poly(M−PS) (e.g., M_n 47 × 10^3, M_w/M_n 1.12) and poly(M−PMMA) (e.g., M_n 30 × 10^3, M_w/M_n 1.16) with narrow MWDs were obtained with an Rh-based living polymerization catalyst [Rh-**2**]. The present polymer brushes were yellow to orange due to the conjugated main chain, and soluble in many solvents including toluene and $CHCl_3$. According to atomic force microscopy (AFM), the single molecules of Rh-**1**-based poly(M−PMMA) were large and diverse in size and wormlike in shape, while those of Rh-**2**-based counterparts were smaller and uniform.

Introduction

Cylindrical polymer brush, also named molecular bottlebrush, refers to one-dimensional polymer brush with a long linear polymer main chain and densely grafted side chains.[1−3] Cylindrical polymer brushes have received considerable attention due to their unique properties both in solution[4] and in bulk,[5] as well as their potential applications in the preparation of nanowires,[6] molecular activators,[7] and crystallization modifiers.[8] Since the pioneering work by Tsukahara et al.[9,10] on the homopolymerization of methacryloyl end-functionalized polystyrene (PS) macromonomers to yield extremely high molecular weight poly(macromonomers), several chemically different poly(macromonomers) such as those based on a poly(methyl methacrylate) (PMMA) main chain and poly(ethylene oxide) (PEO),[11] poly(2-vinylpyridine),[12] and PMMA[13] side chains were successfully synthesized with the macromonomer technique. The traditional chemical pathway to cylindrical polymer brushes is the free radical homopolymerization of macromonomers. It has been difficult, however, to synthesize such polymers with high degree of polymerization (DP) because of the inherently low concentration of polymerizable groups and the steric hindrance of side chains. Recently, Neiser et al. reported the polymerization of methacrylates with oligostyryl side chains using organolanthanide initiators to give polymer brushes with DPs above 500.[14] Aiming at the synthesis of better-defined polymer brushes, ring-opening metathesis polymerization,[15] living anionic polymerization,[16] and atom transfer radical polymerization (ATRP)[17] of macromonomers were examined. Other routes to cylindrical polymer brushes by “grafting from” and “grafting onto” techniques have also been reported, each of which exhibits certain advantages and disadvantages.[1]

Synthesis of novel substituted polyacetylenes is under intensive research,[18,19] and attention has recently focused on novel polymer architectures based on these polymers. Thus, there is growing interest in the polymerization of acetylene-ended macromonomers with Rh catalysts for the purpose to synthesize polyacetylenes possessing linear polymers[20−23] or dendrimers[24−26] as pendants. For example, helical substituted polyacetylenes with helical polypeptide side chains were prepared by the copolymerization of the *N*-propargylamide-terminated peptide-based macromonomer with the alanine-derived *N*-propargylamide.[20] Further, a series of optically active, stereoregular poly(phenylacetylene)s (PPAs) bearing polypeptide chains as grafts were obtained by the polymerization of poly(γ-benzyl-L-glutamate)-based macromonomers having an acetylenic chain end.[21] More recently, a PPA carrying polycarbohydrate ionophores as graft chains was synthesized by the copolymerization of end-functionalized (1→6)-2,5-anhydro-3,4-di-*O*-ethyl-D-glucitol with a 4-ethynylbenzoyl group with phenylacetylene (PA).[22] ATRP is an excellent polymerization technique for the preparation of a broad range of polymers with accurate structural control.[27−30] By using a functional initiator, ATRP is capable of yielding well-defined terminal-functionalized polymers including macromonomers. In our previous work, a propargyl-terminated PS macromonomer was synthesized by ATRP of styrene induced

---

* Corresponding author. E-mail masuda@adv.polym.kyoto-u.ac.jp.

[†] Department of Polymer Chemistry, Graduate School of Engineering, Kyoto University, Katsura Campus.

[‡] Yashima Super-structured Helix Project, Exploratory Research for Advanced Technology (ERATO), Japan Science and Technology Agency (JST).

[§] Department of Molecular Design and Engineering, Graduate School of Engineering, Nagoya University.

10.1021/ma061964z CCC: $37.00

Chart 1. Structures of Atom Transfer Radical Polymerization (ATRP) Initiators, 1 and 2

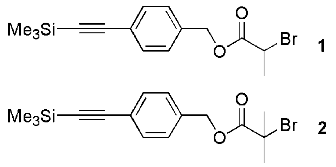

Scheme 1. Synthesis of a PS-Based Macromonomer, M−PS, and Its Poly(macromonomer), Poly(M−PS)

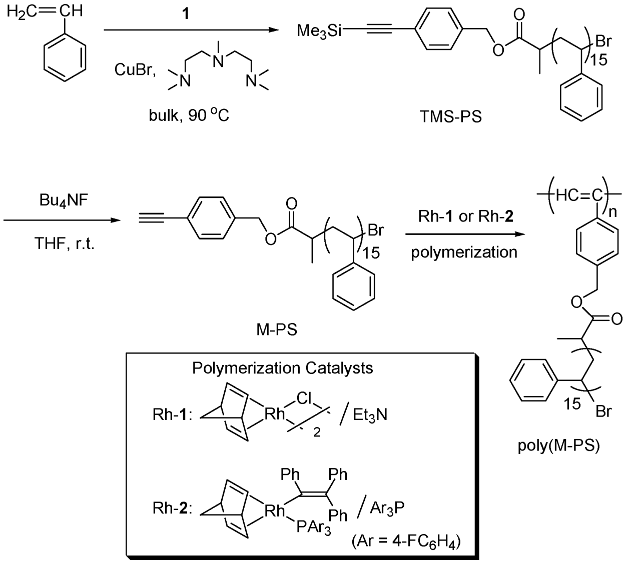

with a functional initiator, propargyl 2-bromopropionate.[23] This macromonomer unfortunately showed only low reactivity toward Rh catalysts, resulting in rather low DPs of 2−6.

As mentioned above, only a few examples of cylindrical polymer brushes with polyacetylene main chains have been known so far, in contrast to relatively many examples of those with vinyl polymer main chains. Because PA exhibits high polymerizability toward Rh catalysts to afford high molecular weight cis-transoidal PPA,[31] PA-terminated vinyl-based macromonomers should homopolymerize well with Rh catalysts to give polymer brushes having high DP main chain. If the PPA main chain has the cis-transoid form, it is expected that the resultant polymer brush would have a centipede-like structure,[32] which consists of a rigid PPA backbone and flexible vinyl polymer side chains. Such a structure may provide unique properties at the nanometer scale.[33]

This paper reports the successful synthesis of cylindrical polymer brushes composed of a highly cis-transoidal PPA main chain and either PS or PMMA side chains, poly(M−PS) and poly(M−PMMA), respectively. These polymer brushes were synthesized by the polymerization of PA-terminated PS and PMMA macromonomers derived from **1** and **2** (Chart 1), respectively, which are abbreviated as M−PS and M−PMMA (Schemes 1 and 2). Polymer brushes possessing high molecular weights were obtained by using a binary Rh catalyst, while those with relatively narrow molecular weight distributions (MWD) (M_w/M_n 1.12−1.16) were synthesized with an Rh-based living polymerization catalyst.

Results and Discussion

Synthesis of Macromonomers. The PS-based macromonomer M−PS (M_n = 1830, M_w/M_n = 1.18, $DP_{n,PS}$ (number-average degree of polymerization) = 15) was prepared by a two-step procedure. First, the acetylene-functionalized ATRP initiator **1** was used to initiate styrene in the presence of CuBr/*N,N,N′,N″,N″*-pentamethyldiethylenetriamine (PMDETA) to afford PS containing a terminal trimethylsilyl (TMS) group, namely, TMS−PS.[34] The acetylene functionality of **1** was protected with the TMS group in order to circumvent complexation with the copper catalyst during polymerization.[35] In the next step, the complete desilylation of TMS−PS using tetrabutylammonium fluoride gave the PS-based macromonomer containing a terminal PA unit, M−PS. In a similar way, PMMA with an end TMS group (TMS−PMMA) was prepared by ATRP of methyl methacrylate using initiator **2**.[35] Subsequent removal of the TMS group in TMS−PMMA in the presence of Na_2CO_3 produced the PMMA-based macromonomer, M−PMMA (M_n = 1860, M_w/M_n = 1.17, $DP_{n,PMMA}$ = 16). The structures of M−PS and M−PMMA were confirmed by ^1H NMR and IR spectra (see Experimental Section).

Scheme 2. Synthesis of a PMMA-Based Macromonomer, M−PMMA, and Its Poly(macromonomer), Poly(M−PMMA)

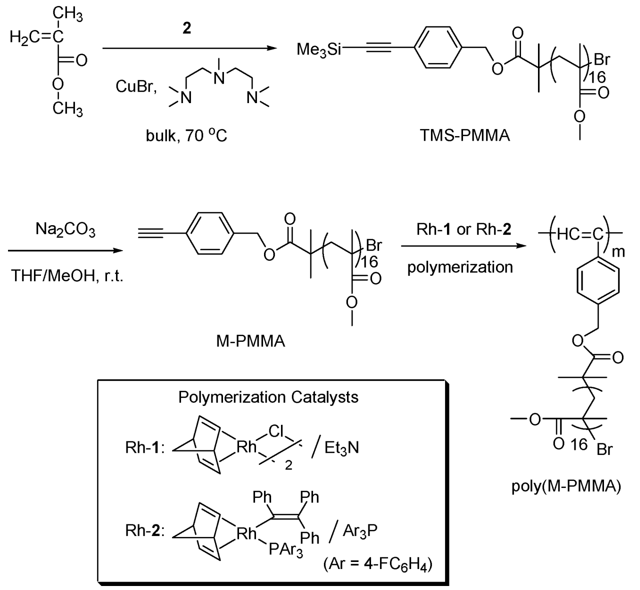

Polymerization of Macromonomers. Polymerization of the PS macromonomer, M−PS, was at first examined by using a typical binary Rh catalyst, $[(nbd)RhCl]_2/Et_3N$ (nbd = 2,5-norbornadiene), denoted by catalyst Rh-**1** in this paper. The concentration of M−PS in the feed was set to be 0.050 M, because the polymerization reaction rapidly formed red gel in 0.10 M of a monomer concentration. The polymerization in 0.050 M solution proceeded homogeneously and the solution became red and viscous over time. The results of polymerization of M−PS with Rh-**1** in toluene are summarized in Table 1. As seen in run 1, the polymerization at 30 °C for 1 h gave poly(M−PS) in good yield (72%) having a high molecular weight ($M_n = 264 \times 10^3$) and an MWD of usual magnitude (M_w/M_n = 2.25) according to gel permeation chromatography (GPC) analysis. Increasing the polymerization time from 1 to 6 h improved both polymer yield (91%) and M_n (296×10^3) to some extent (run 3), but further extension of time was ineffective. At 0 °C, the polymerization of M−PS gave a product insoluble in any common organic solvent (run 5). The polymerization at a high temperature of 60 °C resulted in the formation of poly(M−PS) with a somewhat low polymer yield (64%) and M_n (175×10^3) (run 6). This is probably due to the slight deactivation of the active species at high temperature.

The apparent molecular weight of polymer brushes determined by GPC using a PS calibration is much smaller than their true value owing to rather compact structures. Thus, the

Table 1. Polymerization of PS-Based Macromonomer M−PS (M_n = 1830, M_w/M_n = 1.18), with Rh-1[a]

				poly(M−PS)[b]					
				GPC				GPC−RALLS	
run	temp (°C)	time (h)	yield (%)	$M_n \times 10^{-3\,c}$	$M_w \times 10^{-3\,c}$	M_w/M_n[c]	DP_n[d]	$M_w \times 10^{-3\,e}$	DP_w[f]
1	30	1	72	264	594	2.25	144	1660	769
2	30	3	83	259	525	2.03	141	1730	801
3	30	6	91	296	666	2.25	161	1880	870
4	30	24	87	277	271	4.59	151	1710	792
5	0	6	78	-[g]	-[g]	-[g]	-[g]	-[g]	-[g]
6	60	6	64	175	257	1.47	95	1150	532

[a] Conditions: Rh-**1** = $[(nbd)RhCl]_2/Et_3N$, [M−PS] = 0.050 M, [Rh] = 1.0 mM, $[Et_3N]$ = 10 mM, in toluene. [b] Methanol- and acetone-insoluble product. [c] Main peak (area ratio ~95%) of bimodal gel permeation chromatography (GPC) traces (linear PS standards). The other was a low-molecular-weight oligomer peak (M_n ~10 × 10^3, area ratio ~5%). [d] Number-average degree of polymerization (calculated by M_n/1830). [e] Measured by right-angle laser light scattering (RALLS). [f] Weight-average degree of polymerization (calculated by $M_{w,RALLS}/M_{w,M-PS}$, $M_{w,M-PS}$ = 2160). [g] Insoluble in any organic solvent.

Table 2. Polymerization of PS-Based Macromonomer M−PS (M_n = 1830, M_w/M_n = 1.18), with Rh-2[a]

			poly(M−PS)[b]					
			GPC				GPC−RALLS	
run	time (h)	yield (%)	$M_n \times 10^{-3}$	$M_w \times 10^{-3}$	M_w/M_n	DP_n[c]	$M_w \times 10^{-3\,d}$	DP_w[e]
1	1	78	47	53	1.12	26	93	43
2	3	80	54	63	1.16	29	99	47
3	6	87	109	133	1.22	59	363	168
4	24	93	120	168	1.40	65	508	235

[a] Conditions: Rh-**2** = $[Rh\{C(Ph) = CPh_2\}(nbd)\{P(4\text{-}FC_6H_4)_3\}]/(4\text{-}FC_6H_4)_3P$, [M−PS] = 0.050 M, [Rh] = 1.0 mM, $[(4\text{-}FC_6H_4)_3P]$ = 5.0 mM, at 30 °C in toluene. [b] Methanol- and acetone-insoluble product. [c] Number-average degree of polymerization (calculated by M_n/1830). [d] Measured by right-angle laser light scattering (RALLS). [e] Weight-average degree of polymerization (calculated by $M_{w,\ RALLS}/M_{w,M-PS}$, $M_{w,M-PS}$ = 2160).

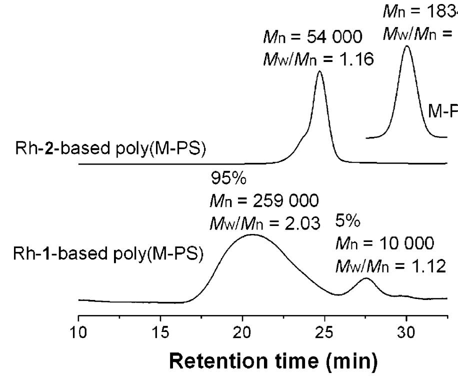

Figure 1. GPC curves of M−PS, Rh-**1**-based poly(M−PS) (run 2, Table 1) and Rh-**2**-based poly(M−PS) (run 2, Table 2) using THF as an eluent with linear PS standards.

Table 3. Polymerization of PMMA-Based Macromonomer M−PMMA (M_n = 1860, M_w/M_n = 1.17), with Rh-1[a]

				poly(M−PMMA)[b]					
				GPC				GPC−RALLS	
run	temp (°C)	time (h)	yield (%)	$M_n \times 10^{-3\,c}$	$M_w \times 10^{-3\,c}$	M_w/M_n[c]	DP_n[d]	$M_w \times 10^{-3\,e}$	DP_w[f]
1	30	1	78	230	460	2.00	124	1480	679
2	30	3	80	239	645	2.70	129	2020	926
3	30	6	80	262	741	2.83	141	2740	1259
4	30	24	82	234	674	2.88	126	2180	1000
5	0	6	91	353	1257	3.56	190	2020	927
6	60	6	71	106	153	1.44	57	432	198

[a] Conditions: Rh-**1** = $[(nbd)RhCl]_2/Et_3N$, [M−PMMA] = 0.050 M, [Rh] = 1.0 mM, $[Et_3N]$ = 10 mM, in toluene. [b] Diethyl ether-insoluble product. [c] Main peak (area ratio ~95%) of bimodal gel permeation chromatography (GPC) traces (linear PS standards). The other was a low-molecular-weight oligomer peak (M_n ~10 × 10^3, area ratio ~5%). [d] Number-average degree of polymerization (calculated by M_n/1860). [e] Measured by right-angle laser light scattering (RALLS). [f] Weight-average degree of polymerization (calculated by $M_{w,RALLS}/M_{w,M-PMMA}$, $M_{w,M-PMMA}$ = 2180).

GPC−RALLS (RALLS: right-angle laser light scattering) method was employed to obtain absolute M_w values. As a result, all the polymers in Table 1 showed absolute molecular weights higher than the GPC values. For example, the polymer of run 1 in Table 1 showed an absolute M_w value of 1660 × 10^3, which is ca. 2.8 times as large as the GPC value. Interestingly, this M_w value corresponds to a weight-average degree of polymerization (DP_w) of PPA chain up to 769.

The effect of polymerization solvents was studied (see Table S1 in Supporting Information), indicating toluene gave higher DP_n of the product than do the other solvents such as benzene, anisole, *o*-dichlorobenzene, CH_2Cl_2, $CHCl_3$, and THF.

It has been reported that binary catalyst composed of $[Rh\{C(Ph){=}CPh_2\}(nbd)\{P(4\text{-}FC_6H_4)_3\}]$ and $(4\text{-}FC_6H_4)_3P$ in 1:5 mole ratio, namely Rh-**2** catalyst, mediates the living polymerization of PA to afford polymer with controlled molecular weight and narrow MWD.[36] Thus, this catalyst system was examined (Table 2). With increasing time, both polymer yield and M_n (GPC) increased from 78% to 93% and 47 × 10^3 to 120 × 10^3, respectively, while the M_w/M_n values (GPC) remained fairly small (1.12−1.40). GPC−RALLS data of runs 1 and 2 showed that these polymers have absolute M_w values in the range of 93 × 10^3 −508 × 10^3 and DP_w values of 43−235. It is noted that this poly(M−PS) has uniform molecular weights with respect to both main chain and graft.

The GPC traces of M−PS and poly(M−PS) observed using linear PS standards are presented in Figure 1. The Rh-**1**-based poly(M−PS) exhibited a bimodal trace shifted to high molecular weight regions compared to that of M−PS, indicating that the resultant polymer consists of two fractions, namely, a high molecular weight polymer (~95%) and a low molecular weight polymer (~5%). In contrast, the GPC trace of Rh-**2**-based poly(M−PS) was much sharper and was practically monomodal.

Results of the polymerization of M−PMMA using Rh-**1** are listed in Table 3. It can be seen from runs 1−4 that M−PMMA also polymerized well with Rh-**1** in toluene at 30 °C, affording poly(M−PMMA) with high molecular weights (M_n = 230 × 10^3 − 262 × 10^3) and usual MWDs (M_w/M_n = 2.00−2.88). The yield and M_n of poly(M−PMMA) were hardly affected by changing the reaction time in the range of 1−24 h, indicating that the polymerization is almost finished within 1 h. Unlike the case of poly(M−PS), the polymerization of M−PMMA at 0 °C provided a soluble polymer having the highest molecular weight (M_n = 353 × 10^3) in the present study in an excellent yield (91%) (run 5). By contrast, raising the temperature to 60 °C, both M_n and yield decreased to 106 × 10^3 and 71%, respectively.

Solvent effects for the polymerization of M−PMMA were also studied and as in the case of polymerization of M−PS, toluene was the best solvent with respect to the DP_n of the product (see Table S2 in Supporting Information).

The polymerization of M−PMMA catalyzed by Rh-**2** afforded well-defined poly(M−PMMA), which possessed lower molecular weights (M_n = 30 × 10^3−58 × 10^3) and relatively narrow MWDs (M_w/M_n = 1.16−1.29) according to GPC (Table

Table 4. Polymerization of PMMA -Based Macromonomer M-PMMA (M_n = 1860, M_w/M_n = 1.17), with Rh-2[a]

		poly(M-PMMA)[b]						
			GPC				GPC−RALLS	
run	time (h)	yield (%)	$M_n \times 10^{-3}$	$M_w \times 10^{-3}$	M_w/M_n	DP_n[c]	$M_w \times 10^{-3}$[d]	DP_w[e]
1	1	82	30	35	1.16	16	62	28
2	3	84	33	39	1.18	16	70	32
3	6	94	58	75	1.29	31	164	22
4	24	96	38	46	1.20	20	95	43

[a] Conditions: Rh-**2** = [Rh{C(Ph)=CPh$_2$}(nbd){P(4-FC$_6$H$_4$)$_3$}]/(4-FC$_6$H$_4$)$_3$P, [M−PMMA] = 0.050 M, [Rh] = 1.0 mM, and [(4-FC$_6$H$_4$)$_3$P] = 5.0 mM, at 30 °C in toluene. [b] Diethyl ether-insoluble product. [c] Number-average degree of polymerization (calculated by M_n/1860). [d] Measured by right-angle laser light scattering (RALLS). [e] Weight-average degree of polymerization (calculated by $M_{w,RALLS}/M_{w,M-PMMA}$, $M_{w,M-PMMA}$ = 2180).

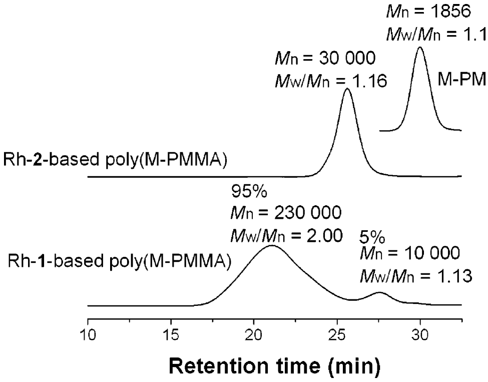

Figure 2. GPC curves of M−PMMA, Rh-**1**-based poly(M−PMMA) (run 1, Table 3) and Rh-**2**-based poly(M−PMMA) (run 1, Table 4) using THF as an eluent with linear PS standards.

4). Although both yield and M_n increased with time in the range of 1−24 h, it is noted that the polymerization proceeds very fast within 1 h. The GPC traces of Rh-**1**- and Rh-**2**-based poly(M−PMMA)s displayed similar patterns to those of poly(M−PS)s, as seen in Figure 2. As in the case of poly(M−PS), GPC−RALLS analysis of poly(M−PMMA)s given by Rh-**1** and Rh-**2** showed the higher molecular weight comparing to the results of GPC measurement.

We synthesized PA-terminated macromonomers having a longer PS or PMMA chain ($DP_{n,PS}$ or $DP_{n,PMMA}$ above 35), and attempted their polymerization by using Rh-**1**. However, these macromonomers only produced poly(macromonomers) with multimodal GPC traces and low DPs of less than 15 in the main chain. This is probaly due to the steric hindrance of too long and bulky substituents.

Characterization and Properties of the Polymer Brushes. The structures of the formed poly(macromonomers) were elucidated by infrared spectra (IR) and ^{1}H NMR spectroscopies. The IR spectra of both M−PS and M−PMMA exhibited absorption peaks at 3288 and 3265 cm^{-1}, respectively, due to the ≡C−H stretching vibration, which disappeared in the spectra of their poly(macromonomers), suggesting that the polymerization of the triple bond of the macromonomers occurred properly. According to ^{1}H NMR spectra (Figures 3 and 4), the resonances of acetylenic proton in macromonomers, M−PS (3.08 ppm) and M−PMMA (3.10 ppm), completely disappeared in the polymers. Highly stereoregular cis-transoidal PPAs are known to display a sharp signal at 5−7 ppm due to the olefinic proton in the main chain.[37,38] However, the cis olefinic proton signal was not observed in the ^{1}H NMR spectra of the present poly(macromonomers), so the stereoregularity of their main chain could not be determined. This tendency is similar to recently reported polymers from polypeptide-based macromonomers carrying PA chain end group.[21] The low mobility of PPA main chain should be responsible, and thus laser Raman analysis was performed in order to elucidate the stereoregularity.[39] Table S3 (see Supporting Information) summarizes results of the laser Raman spectra of the Rh-**1**-based poly(M−PS) and poly(M−PMMA) measured in both solid state and solutions (CHCl$_3$ and THF). The Raman spectra of both samples exhibited intense characteristic peaks at 1539−1574 cm^{-1} (C=C stretching), 1343−1337 cm^{-1} (C−C stretching) and 886−907 cm^{-1} (C−H deformation) based on the *cis*-polyacetylene structure (Figures S1−S6). In contrast, no clear peaks due to the trans structure were detected in these spectra, thus indicative of highly cis-transoidal structures of Rh-**1**-based poly(macromonomers). It

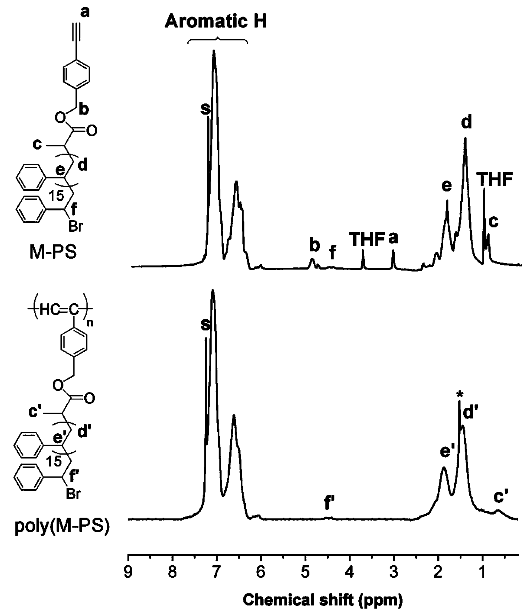

Figure 3. ^{1}H NMR spectra of M−PS and poly(M−PS) (run 2, Table 1) (s, solvent; ∗, H$_2$O).

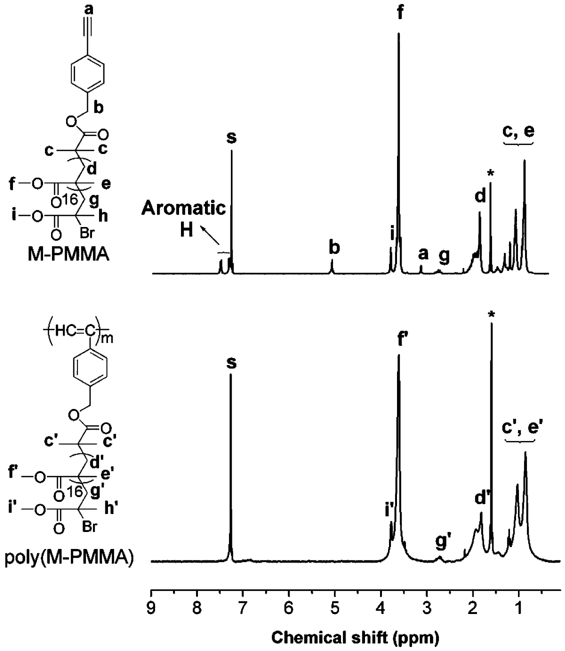

Figure 4. ^{1}H NMR spectra of M−PMMA and poly(M−PMMA) (run 1, Table 3) (s, solvent; ∗, H$_2$O).

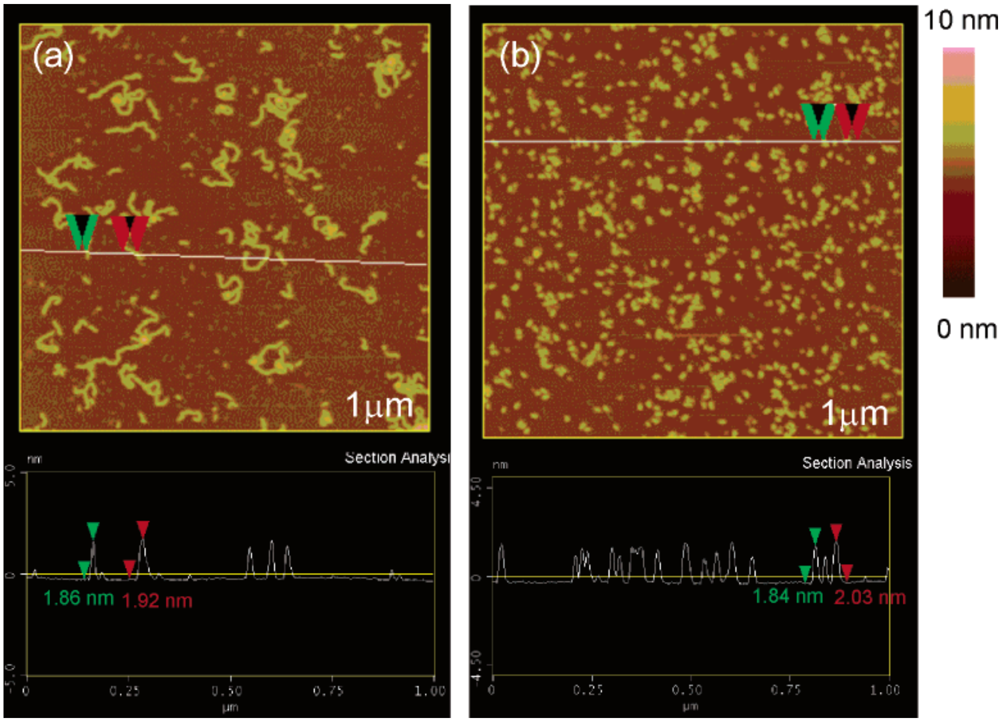

Figure 5. AFM height images of (a) Rh-**1**-based poly(M−PMMA) (run 2, Table 3) (ca. 1.86−1.92 nm in height) and (b) Rh-**2**-based poly(M−PMMA) (run 3, Table 4) (ca. 1.84−2.03 nm in height). Samples were prepared by spin-casting a drop of polymers in benzene (2×10^{-5} g/mL). The figures correspond to an area of 1 μm × 1 μm.

is presumed that the Rh-**2**-based ones are also highly cis-transoidal.[40]

M−PS was soluble in *N*,*N*-dimethylformamide (DMF), ethyl acetate, $CHCl_3$, THF, toluene, benzene, acetone and diethyl ether, while its polymerization product, poly(M−PS), became insoluble in acetone and diethyl ether. M−PMMA displayed similar solubility to M−PS. After polymerization of M−PMMA, the resulting polymer became insoluble in diethyl ether. The Rh-**1**-based poly(M−PS) and poly(M−PMMA) were yellow solids, while the Rh-**2**-based polymers were orange solids. All the poly(macromonomers) showed UV−vis absorptions in the range of 360−600 nm, whose maxima were located from 423 to 454 nm, which are attributable to the conjugated main chain (Figure S7).

Thermogravimetric analysis (TGA) revealed that poly(M−PS) and poly(M−PMMA) were thermally stable up to 150 °C in air. It is noteworthy that poly(M−PS) and poly(M−PMMA) displayed very good stability in solution as compared to PPAs. Most of the polymers from monosubstituted PAs readily decompose in solution, and the degradation is extremely rapid in THF. For example, the M_n of PPA decreases from 523×10^3 to 42×10^3 within 5 h in THF.[41] By contrast, the degradation of the present poly(macromonomers) was much slower. For instance, Rh-**1**-based poly(M−PS) with initial M_n of 259×10^3 maintained relatively high molecular weight ($M_n = 182 \times 10^3$) and the M_n of Rh-**2**-based poly(M−PS) slightly decreased from 47×10^3 to 45×10^3 even after they were stored in THF for 24 h, and poly(M−PMMA) had similar stability in solution to poly(M−PS). This enhanced stability probably originates from the presence of long and bulky graft chains, which help to stabilize the PPA main chain against the degradation.

To visualize single molecules of the present polymers by atomic force microscopy (AFM), poly(M−PS) and poly(M−PMMA) were dissolved in benzene at low concentration ($c = 2 \times 10^{-5}$ g/mL), and spin-cast onto mica. AFM images of poly(M−PS) showed the monolayer island formation, which was frequently observed for PS-based poly(macromonomers) because of the low affinity of PS to mica.[42] On the other hand, single molecules of Rh-**1**-based poly(M−PMMA) were clearly identified by AFM height image (ca. 1.86−1.92 nm in height) thanks to the sufficient affinity of PMMA to mica (Figure 5a). Interestingly, this high molecular weight cylindrical polymer brush adopts wormlike conformation, similarly to the poly(macromonomers) composed of a PMMA main chain and relatively short PMMA side chains (apparent M_w of the whole polymer 7.5×10^6 to 60×10^6; M_n of side chain 2410),[43] and its chain is not so rigid as the chain of poly(macromonomer) consisting of a PMMA main chain and longer poly(ϵ-caprolactone)-*block*-poly(*n*-butyl acrylate) side chains [absolute M_n of the whole polymer 10.9×10^6; DP_n of poly(ϵ-caprolactone) 35; DP_n of poly(*n*-butyl acrylate) 110].[44] The AFM profile also manifests that the length of the of Rh-**1**-based poly(M−PMMA) molecule is diverse with one another. In contrast, the AFM figure of the Rh-**2**-based poly(M−PMMA) is characterized by relatively short molecules with high uniformity in length, which shows in the range of same height as Rh-**1**-based product (Figure 5b). This observation is quite consistent with its lower molecular weight as well as narrow MWD.

Conclusions

The Rh-catalyzed polymerization of PS and PMMA macromonomers terminated with PA yielded novel cylindrical brushes, poly(M−PS) and poly(M−PMMA), respectively. Use of two different Rh catalysts provided polymer brushes with different DPs and MWDs. Single molecules of poly(M−PMMA)s were clearly visualized by AFM. These single molecules showed coiled wormlike conformation, indicating that the main chain was not very rigid. To the best of our knowledge, poly(M−PS) and poly(M−PMMA) are the first examples of cylindrical polymer brushes that consist of a conjugated polyene main chain and vinyl polymer side chains. We anticipate that many new and unique polymer brushes bearing the PPA main chain can be synthesized by the macromonomer strategy.

Experimental Section

Materials. Styrene (Wako, Japan; 98%) and methyl methacrylate (MMA) (Wako, Japan; 98%) monomers were dried over $\mathrm{CaCl_2}$ overnight and distilled twice from $\mathrm{CaH_2}$ under reduced pressure. CuBr (Aldrich, 98%), *N*,*N*,*N*′,*N*″,*N*″-pentamethyldiethylenetriamine (PMDETA) (Wako, Japan; 98%), 2-bromopropionyl bromide (TCI, Japan; 98%), 2-bromoisobutyryl bromide (TCI, Japan; 98%), tetrabutylammonium fluoride [TCI, Japan; 1.0 M in tetrahydrofuran (THF)], triethylamine ($\mathrm{Et_3N}$) (Wako, Japan; 98%) and $(4\text{-}\mathrm{FC_6H_4})_3\mathrm{P}$ (Aldrich, 99%) were used as received. [4-(Trimethylsilylethynyl)phenyl]methanol,[45] $[(\mathrm{nbd})\mathrm{RhCl}]_2$[46] and $[\mathrm{Rh}\{\mathrm{C(Ph)}{=}\mathrm{CPh_2}\}(\mathrm{nbd})\{\mathrm{P}(4\text{-}\mathrm{FC_6H_4})_3\}]$[33] were synthesized according to the literature. THF and $\mathrm{CHCl_3}$ used in the laser Raman measurements were dried over sodium benzophenone ketyl and $\mathrm{CaH_2}$, respectively, and distilled under nitrogen. These solvents were stored under nitrogen over molecular sieves 4 Å (Nacalai Tesque, Japan). Toluene, benzene, $\mathrm{CH_2Cl_2}$ and $\mathrm{CHCl_3}$ were distilled from $\mathrm{CaH_2}$ under argon. Anisole and *o*-dichlorobenzene were purified by distillation from $\mathrm{CaH_2}$ under reduced pressure. THF used as polymerization solvent was distilled from sodium benzophenone ketyl under argon. Other reagents were commercially obtained and used without further purification.

Measurements. ^{1}H (400 MHz) and ^{13}C NMR (100 MHz) spectra were recorded in chloroform-*d* ($\mathrm{CDCl_3}$) using tetramethylsilane as internal reference ($\delta = 0$) on a JEOL EX-400 spectrometer. The melting points were measured with a Yanaco micro melting point apparatus. Elemental analysis was carried out at the Kyoto University Elemental Analysis Center. Infrared spectra (IR) were recorded on a JASCO FTIR-4100 spectrophotometer with KBr pellets. Laser Raman spectra were taken on a Jasco RMP-200 spectrophotometer. A typical procedure for the measurements in solution is as follows: 1.0 mg of sample was placed in a 100 mL flask equipped with a stopcock and 50 mL of the solvent was added to it. The solution was then transferred to a 1.0 mm glass capillary with a pipet and the ends were sealed. The apparent M_n, M_w, and MWD were determined by gel permeation chromatography (GPC) on a Jasco Gulliver System (PU-980, CO-965, RI-930, and UV-1570) equipped with a series of PS gel columns (Shodex KF805L × 3, bead size: 10 μm, molecular weight range up to 4×10^6, flow rate 1 mL/min), using THF as an eluent at 40 °C with a PS calibration. The absolute molecular weights were determined by GPC conducted in THF at 40 °C using a TOSOH TSK gel column (TSKgel $\mathrm{GMH_{XL}}$, bead size: 9 μm, molecular weight range up to 4×10^8, flow rate 1 mL/min) in series with a triple detection system: a differential refractometer (JASCO RI930), and a Viscotek T60A dual (viscosity and RALLS, wave length 670 nm, output power 7 mW) detector. Samples (5×10^{-4} g/mL in THF) were filtered through 0.2 μm-pore-size membrane filters (TOSOH H-13−2) beforehand, and the injection volume was 200 μL. The absolute molecular weights were calculated using TriSEC software (Viscotek). Because the compositions of PS and PMMA in poly(M−PS) and poly(M−PMMA) were ~95%, the refractive index increment values of PS ($\mathrm{d}n/\mathrm{d}c = 0.184$)[47] and PMMA ($\mathrm{d}n/\mathrm{d}c = 0.886$)[47] were used for the d*n*/d*c* values of poly(M−PS) and poly(M−PMMA), respectively. Samples for AFM measurements were prepared by spin-casting a drop of polymers in benzene (2×10^{-5} g/mL) at room temperature at 1800 rpm on freshly cleaved mica. The AFM measurements were performed using a Nanoscope IV with a multimode AFM unit (Veeco Instruments, Santa Barbara, CA) in air at ambient temperature with standard silicon cantilevers (NCH, NanoWorld, Neuchâtel, Switzerland) in the tapping mode. The AFM images are shown without any image processing except flattening. UV−vis spectra were recorded on a Shimadzu UV-2200 spectrophotometer. Thermogravimetric analysis (TGA) was conducted on a Perkin-Elmer TGA thermal analyzer.

Synthesis of 2-Bromopropionic Acid 4-Trimethylsilylethynylbenzyl Ester (1). Pyridine (2.55 g, 32.2 mmol) and 2-bromopropionyl bromide (4.32 g, 20.0 mmol) were added in sequence to a solution of [4-(trimethylsilylethynyl)phenyl]methanol (4.08 g, 20.0 mmol) in 40 mL of dry THF cooled at 0 °C under an argon atmosphere. The reaction mixture was allowed to warm to room temperature and stirred overnight. The mixture was washed with water, dilute hydrochloric acid, and brine, dried over $\mathrm{MgSO_4}$, and concentrated. The crude product was purified by silica gel column chromatography eluted with hexane/ethyl acetate = 20/1 (volume ratio) to give 2.80 g of **1** as a white solid. Yield: 41.3%. Melting point: 28−29 °C. ^{1}H NMR ($\mathrm{CDCl_3}$, ppm): $\delta = 7.44$ (d, $J = 8.4$ Hz, 2H, $\mathrm{H_{Ar}}$), 7.28 (d, $J = 8.0$ Hz, 2H, $\mathrm{H_{Ar}}$), 5.17 (s, 2H, $\mathrm{C}H_2$), 4.41 (q, $J = 6.8$ Hz, 1H, $\mathrm{C}H\mathrm{(CH_3)Br}$), 1.83 (d, $J = 6.8$ Hz, 3H, $\mathrm{CH(C}H_3\mathrm{)Br}$), 0.23 (s, 9H, $\mathrm{Si(C}H_3)_3$). ^{13}C NMR ($\mathrm{CDCl_3}$, ppm): $\delta = 169.84$ ($C = \mathrm{O}$), 135.37 ($\mathrm{C_{Ar}}$ (*para* to C≡C)), 132.11 (2C, $\mathrm{C_{Ar}}$ (*ortho* to C≡C)), 127.85 (2C, $\mathrm{C_{Ar}}$ (*meta* to C≡C)), 123.25 ($\mathrm{C_{Ar}}$ (*ipso* to C≡C)), 104.50 (C≡*C*−Ar), 94.88 (*C*≡C−Ar), 66.98 ($C\mathrm{H_2}$), 39.83 ($C\mathrm{H(CH_3)Br}$), 21.60 ($\mathrm{CH(}C\mathrm{H_3)Br}$), −0.11 (3C, $\mathrm{Si(}C\mathrm{H_3)_3}$). Anal Calcd for $\mathrm{C_{15}H_{19}BrO_2Si}$ (339.3): C, 53.10; H, 5.64. Found: C, 53.39; H, 5.64.

2-Bromo-2-methylpropionic Acid 4-Trimethylsilanylethynylbenzyl Ester (2). This compound was prepared in a similar way as for **1** except the use of 2-bromoisobutyryl bromide as the starting compound; the product was purified by silica gel column chromatography eluted with hexane/ether acetate = 10/1 (volume ratio) to give 4.20 g of **2** as a white solid. Yield: 59.1%. Melting point: 57−58 °C. ^{1}H NMR ($\mathrm{CDCl_3}$, ppm): $\delta = 7.45$ (d, $J = 7.6$ Hz, 2H, $\mathrm{H_{Ar}}$), 7.31 (d, $J = 7.8$ Hz, 2H, $\mathrm{H_{Ar}}$), 5.18 (s, 2H, $\mathrm{C}H_2$), 1.94 (s, 6H, $\mathrm{C(C}H_3)_2\mathrm{Br}$), 0.25 (s, 9H, $\mathrm{Si(C}H_3)_3$). ^{13}C NMR ($\mathrm{CDCl_3}$, ppm): $\delta = 171.32$ ($C = \mathrm{O}$), 135.64 ($\mathrm{C_{Ar}}$ (*para* to C≡C)), 132.12 (2C, $\mathrm{C_{Ar}}$ (*ortho* to C≡C)), 127.66 (2C, $\mathrm{C_{Ar}}$ (*meta* to C≡C)), 123.16 ($\mathrm{C_{Ar}}$ (*ipso* to C≡C)), 104.55 (C≡*C*−Ar), 94.80 (*C*≡C−Ar), 67.00 ($C\mathrm{H_2}$), 55.47 ($C\mathrm{(CH_3)_2Br}$), 30.67 (2C, $\mathrm{C(}C\mathrm{H_3)_2Br}$), −0.09 (3C, $\mathrm{Si(}C\mathrm{H_3)_3}$). Anal. Calcd for $\mathrm{C_{16}H_{21}BrO_2Si}$ (353.3): C, 54.39; H, 5.99. Found: C, 54.32; H, 5.88.

Synthesis of M—PS. Styrene (9.07 g, 87.2 mmol), **1** (0.740 g, 2.18 mmol), and CuBr (0.156 g, 1.09 mmol) were placed in a 40 mL flask equipped with a three-way stopcock, and the mixture was subjected to three freeze−pump−thaw cycles. The flask was placed in an oil bath preheated to 90 °C, and PMDETA (0.187 g, 1.09 mmol) was added with an argon-purged syringe. After 90 min, the flask was removed from the bath, and opened; the mixture was diluted with THF (7.0 mL), and passed through a neutral alumina column to remove the catalyst. The solution was concentrated to ca. 15 mL by rotary evaporation. The product was precipitated in a large amount of methanol and dried under reduced pressure to give 3.90 g of TMS−PS (Scheme 1) as a white powder. Yield: 42.8%. $M_n = 2410$, $M_w/M_n = 1.19$ (GPC, linear PS standards). ^{1}H NMR ($\mathrm{CDCl_3}$, ppm): $\delta = 7.80{-}6.30$ (broad m, $\mathrm{H_{Ar}}$), 4.89 (broad s, $\mathrm{Ar{-}C}H_2\mathrm{{-}O}$), 4.60−4.35 (broad m, $\mathrm{CH_2{-}C}H\mathrm{(Ph)Br}$), 2.60−1.20 (broad m, $\mathrm{C}H_2$ and $\mathrm{C}H$ of PS chain), 0.93 (broad m, $\mathrm{O_2C{-}CH(C}H_3\mathrm{)CH_2}$), 0.26 (s, $\mathrm{Si(C}H_3)_3$). IR (KBr, $\mathrm{cm^{-1}}$): $\nu = 3025$, 2923, 2157 (C≡C), 1735 (C=O). To remove the trimethylsilyl (TMS) group, TMS−PS (3.90 g, 1.62 mmol) was dissolved in THF (160 mL), and tetrabutylammonium fluoride (21.0 mL, 21.0 mmol) was added. The reaction mixture was stirred overnight at room temperature, and then concentrated to ca. 10 mL by rotary evaporation. The macromonomer was precipitated in a large amount of methanol and dried under reduced pressure to yield 3.44 g of M−PS as a white powder. The ^{1}H NMR spectrum indicated that the deprotection of the TMS group was complete. Yield: 92.7%. $M_n = 1830$, $M_w/M_n = 1.18$ (GPC, linear PS standards). ^{1}H NMR ($\mathrm{CDCl_3}$, ppm): $\delta = 7.80{-}6.30$ (broad m, $\mathrm{H_{Ar}}$), 5.00−4.70 (broad, $\mathrm{Ar{-}C}H_2\mathrm{{-}O}$), 4.60−4.30 (broad m, $\mathrm{CH_2{-}C}H\mathrm{(Ph)Br}$), 3.08 (s, $\mathrm{{\equiv}C{-}}H$), 2.60−1.10 (broad m, $\mathrm{C}H_2$, $\mathrm{C}H$ of PS chain), 0.93 (m, $\mathrm{O_2C{-}CH(C}H_3\mathrm{)CH_2}$). IR (KBr, $\mathrm{cm^{-1}}$): $\nu = 3288$ (≡C−H), 3025, 2923, 1735 (C=O).

Synthesis of M—PMMA. In a manner similar to that used to prepare TMS−PS, ATRP of methyl methacrylate (3.74 g, 32.7 mmol) catalyzed by a mixture of **2** (1.156 g, 0.327 mmol), CuBr (0.235 g, 1.64 mmol), and PMDETA (0.284 g, 1.64 mmol) was carried out at 70 °C for 15 min. The product was precipitated in a large amount of hexane and dried under reduced pressure to give 1.90 g of TMS−PMMA (Scheme 2) as white powder. Yield: 50.8%. $M_n = 2350$, $M_w/M_n = 1.20$ (GPC, linear PS standards). ^{1}H NMR ($CDCl_3$, ppm): $\delta = 7.46-7.30$ (m, H_{Ar}), 5.05 (s, Ar−CH_2−O), 3.82 (s, terminal CO_2CH_3), 3.70−3.50 (broad s, CO_2CH_3 on backbone), 2.80−2.60 (broad, CH_2 of terminal MMA moiety), 2.30−0.60 (broad, CH_2 and CH_3 of backbone), 0.26 (s, Si(CH_3)$_3$). IR (KBr, cm^{-1}): $\nu = 2993$, 2951, 2158 (C≡C), 1729 (C═O). TMS−PMMA (1.82 g, 0.774 mmol) was dissolved in a mixture of THF (20 mL) and methanol (20 mL), and Na_2CO_3 (1.00 g, 9.43 mmol) was added. The reaction mixture was stirred overnight at room temperature and then concentrated to ca. 5.0 mL by rotary evaporation. The macromonomer was precipitated in a large amount of hexane and dried under reduced pressure to yield 1.42 g of M−PMMA as a white powder. The complete removal of the TMS group was confirmed by the ^{1}H NMR spectrum. Yield: 78.9%. $M_n = 1860$, $M_w/M_n = 1.17$ (GPC, linear PS standards). ^{1}H NMR ($CDCl_3$, ppm): $\delta = 7.46-7.30$ (m, H_{Ar}), 5.06 (s, Ar−CH_2−O), 3.76 (s, terminal CO_2CH_3), 3.70−3.50 (broad s, CO_2CH_3 on backbone), 3.10 (s, ≡C−H), 2.80−2.60 (broad s, CH_2 of terminal MMA moiety), 2.30−0.60 (broad m, CH_2 and CH_3 of backbone). IR (KBr, cm^{-1}): $\nu = 3265$ (≡C−H), 2993, 2950, 1731 (C═O).

Polymerization of M−PS. The polymerization using [(nbd)-RhCl]$_2$/Et$_3$N was carried out under the following conditions: [M−PS] = 0.050 M, [Rh] = 1.0 mM, and [Et$_3$N] = 10 mM. A typical procedure is as follows (run 1, Table 1): A solution of [(nbd)RhCl]$_2$ and Et$_3$N in a distilled solvent was added to a solution of M−PS in the same solvent under argon. After being vigorously stirred for 1 h at 30 °C, the solution was poured into a large amount of methanol to precipitate the polymers. The resultant polymer was collected, filtered, washed with acetone to remove the unreacted macromonomer [acetone is a solvent of M−PS but is a nonsolvent of poly(M−PS)], and dried under reduced pressure until constant weight. Yield: 72%. $M_n = 264 \times 10^3$, $M_w/M_n = 2.25$ (GPC, linear PS standards). ^{1}H NMR ($CDCl_3$, ppm): $\delta = 7.80-6.30$ (broad m, H_{Ar}), 4.60−4.30 (broad m, CH_2−CH(Ph)Br), 2.60−1.10 (broad m, CH_2 and CH of PS chain), 0.72 (broad s, CH_3). The signals assigned to olefinic protons on main chain and benzyl protons were not observed probably due to their broadness. The polymerization catalyzed by living catalyst system, [Rh{C(Ph)═CPh$_2$}(nbd){P(4-FC$_6$H$_4$)$_3$}]/(4-FC$_6$H$_4$)$_3$P, was carried out under the following conditions: [M−PS] = 0.050 M, [Rh] = 1.0 mM, and [(4-FC$_6$H$_4$)$_3$P] = 5.0 mM. The procedure was similar to that of [(nbd)RhCl]$_2$/Et$_3$N-catalyzed polymerization. The ^{1}H NMR spectra of the obtained polymers were similar to that of [(nbd)RhCl]$_2$/Et$_3$N-catalyzed poly(M−PS).

Polymerization of M−PMMA. M−PMMA was polymerized in a similar manner to M−PS by using either [(nbd)RhCl]$_2$/Et$_3$N or [Rh{C(Ph)═CPh$_2$}(nbd){P(4-FC$_6$H$_4$)$_3$}]/(4-FC$_6$H$_4$)$_3$P, except that the polymerization solution was poured into diethyl ether to precipitate poly(M−PMMA), which was separated from unreacted M−PMMA because the latter was soluble in diethyl ether. The resulting polymer was collected, filtered, and dried under reduced pressure until constant weight. The characterization results of an example poly(M−PMMA) (run 1, Table 3) are as follows: Yield: 78%. $M_n = 230 \times 10^3$, $M_w/M_n = 2.00$ (GPC, linear PS standards). ^{1}H NMR ($CDCl_3$, ppm): $\delta = 3.76$ (s, terminal CO_2CH_3), 3.70−3.50 (broad s, CO_2CH_3 on backbone), 2.80−2.60 (s, CH_2 of terminal MMA moiety), 2.40−0.50 (broad m, CH_2 and CH_3 of backbone). The signals assigned to olefinic protons on main chain and benzyl protons were not observed probably due to their broadness.

Acknowledgment. W.Z. acknowledges a scholarship from the Ministry of Education, Culture, Sports, Science, and Technology, Japan.

Supporting Information Available: Tables giving solvent effects on polymerization (Tables S1 and S2) and Raman shifts (Table S3) and figures showing laser Raman spectra (Figures S1−S6) and UV−vis spectra (Figure S7). This material is available free of charge via the Internet at http://pubs.acs.org.

References and Notes

(1) Zhang, M.; Mueller, A. H. E. *J. Polym. Sci., Part A: Polym. Chem.* **2005**, *43*, 3461−3481.

(2) Hadjichristidis, N.; Pitsikalis, M.; Iatrou, H.; Pispas, S. *Macromol. Rapid Commun.* **2003**, *24*, 979−1013.

(3) Ito, K.; Kawaguchi, S. *Adv. Polym. Sci.* **1999**, *142*, 129−178.

(4) Ito, K.; Tomi, Y.; Kawaguchi, S. *Macromolecules* **1992**, *25*, 1534−1538.

(5) Tsukahara, Y.; Ohta, Y.; Senoo, K. *Polymer* **1995**, *36*, 3413−3416.

(6) Djalali, R.; Li, S. Y.; Schmidt, M. *Macromolecules* **2002**, *35*, 4282−4288.

(7) Li, C.; Gunari, N.; Fischer, K.; Janshoff, A.; Schmidt, M. *Angew. Chem., Int. Ed.* **2004**, *43*, 1101−1104.

(8) He, L.; Zhang, Y.; Ren, L.; Chen, L.; Wei, H.; Wang, D. *Macromol. Chem. Phys.* **2006**, *207*, 684−693.

(9) Tsukahara, Y.; Mizuno, K.; Segawa, A.; Yamashita, Y. *Macromolecules* **1989**, *22*, 1546−1552.

(10) Tsukahara, Y.; Tsutsumi, K.; Yamashita, Y.; Shimada, S. *Macromolecules* **1990**, *23*, 5201−5208.

(11) Ito, K.; Tanaka, K.; Tanaka, H.; Imai, G.; Kawaguchi, S.; Itsuno, S. *Macromolecules* **1991**, *24*, 2348−2354.

(12) Dziezok, P.; Sheiko, S. S.; Fischer, K.; Schmidt, M.; Moller, M. *Angew. Chem., Int. Ed. Engl.* **1997**, *36*, 2812−2815.

(13) Radke, W.; Muller, A. H. E. *Makromol. Chem., Macromol. Symp.* **1992**, *54/55*, 583−594.

(14) Neiser, M. W.; Okuda, J.; Schmidt, M. *Macromolecules* **2003**, *36*, 5437−5439.

(15) Morandi, G.; Montembault, V.; Pascual, S.; Legoupy, S.; Fontaine, L. *Macromolecules* **2006**, *39*, 2732−2735.

(16) Pantazis, D.; Chalari, I.; Hadjichristidis, N. *Macromolecules* **2003**, *36*, 3783−3785.

(17) Yamada, K.; Miyazaki, M.; Ohno, K.; Fukuda, T.; Minoda, M. *Macromolecules* **1999**, *32*, 290−293.

(18) Lam, J. W. Y.; Tang, B. Z. *Acc. Chem. Res.* **2005**, *38*, 745−754.

(19) Masuda, T.; Sanda, F. In *Handbook of Metathesis*; Grubbs, R. H., Ed.; Wiley-VCH: Weinheim, Germany, 2003; Vol. 3, Chapter 3.11.

(20) Sanda, F.; Gao, G. Z.; Masuda, T. *Macromol. Biosci.* **2004**, *4*, 570−574.

(21) Maeda, K.; Kamiya, N.; Yashima, E. *Chem.−Eur. J.* **2004**, *10*, 4000−4010.

(22) Otsuka, I.; Sakai, R.; Satoh, T.; Kakuchi, R.; Kaga, H.; Kakuchi, T. *J. Polym. Sci., Part A: Polym. Chem.* **2005**, *43*, 5855−5863.

(23) Zhang, W.; Shiotsuki, M.; Masuda, T. *Macromol. Chem. Phys.* **2006**, *207*, 933−940.

(24) Percec, V.; Rudick, J. G.; Peterca, M.; Wagner, M.; Obata, M.; Mitchell, C. M.; Cho, W. D.; Balagurusamy, V. S. K.; Heiney, P. A. *J. Am. Chem. Soc.* **2005**, *127*, 15257−15264.

(25) Kaneko, T.; Horie, T.; Asano, M.; Aoki, T.; Oikawa, E. *Macromolecules* **1997**, *30*, 3118−3121.

(26) Kaneko, T.; Yamamoto, K.; Asano, M.; Teraguchi, M.; Aoki, T. *J. Membr. Sci.* **2006**, *278*, 365−372.

(27) Matyjaszewski, K. *Prog. Polym. Sci.* **2005**, *30*, 858−875.

(28) Matyjaszewski, K., Ed. *Advances in Controlled/Living Radical Polymerization*; American Chemical Society: Washington, DC, 2003.

(29) Matyjaszewski, K.; Xia, J. *Chem. Rev.* **2001**, *101*, 2921−2990.

(30) Coessens, V.; Pintauer, T.; Matyjaszewski, K. *Prog. Polym. Sci.* **2001**, *26*, 337−377.

(31) Yang, W.; Tabata, M.; Yokota, K.; Shimizu, A. *Polym. J.* **1991**, *23*, 1135−1138.

(32) Iatrou, H.; Mays, J. W.; Hadjichristidis, N. *Macromolecules* **1998**, *31*, 6697−6701.

(33) Schappacher, M.; Deffieux, A. *Macromolecules* **2005**, *38*, 7209−7213.

(34) Lutz, J.-F.; Borner, H. G.; Weichenhan, K. *Makromol. Rapid. Commun.* **2005**, *26*, 514−518.

(35) Opsteen, J. A.; van Hest, C. J. *Chem. Commun.* **2005**, 57−59.

(36) Miyake, M.; Misumi, Y.; Masuda, T. *Macromolecules* **2000**, *33*, 6636−6639.

(37) Simionescu, C. I.; Dumitrescu, S.; Percec, V. *J. Polym. Sci., Polym. Symp.* **1978**, *64*, 209−227.

(38) Furlani, A.; Napoletano, C.; Russo, M. V.; Feast, W. J. *Polym. Bull. (Berlin)*. **1986**, *16*, 311−317.

(39) Tabata, M.; Tanaka, Y.; Sadahiro, Y.; Sone, T.; Yokota, K.; Miura, I. *Macromolecules* **1997**, *30*, 5200−5204.

(40) Abdul Karim, S. M.; Nomura, R.; Masuda, T. *J. Polym. Sci., Part A: Polym. Chem.* **2002**, *40*, 2458−2463.

(41) Sedlacek, J.; Vohlidal, J.; Grubisic-Gallot, Z. *Makromol. Chem., Rapid. Commun.* **1993**, *14*, 51−53.

(42) Sheiko, S. S.; Gerle, M.; Fischer, K.; Schmidt, M.; Moller, M. *Langmuir* **1997**, *13*, 5368−5372.

(43) Gerle, M.; Fischer, K.; Roos, S.; Muller, A. H. E.; Schmidt, M.; Sheiko, S. S.; Prokhorova, S.; Moller, M. *Macromolecules* **1999**, *32*, 2629−2637.

(44) Lee, H.-i.; Jakubowski, W.; Matyjaszewski, K.; Yu, S.; Sheiko, S. S. *Macromolecules* **2006**, *39*, 4983−4989.
(45) Teraguchi, M.; Mottate, K.; Kim, S. Y.; Aoki, T.; Kaneko, T.; Hadano, S.; Masuda, T. *Macromolecules* **2005**, *38*, 6367−6373.
(46) Schrock, R. R. *J. Am. Chem. Soc.* **1971**, *93*, 2397−2407.
(47) *Polymer Handbook*, 3rd ed.; Brandrup, J., Immergut, E. H., Eds.; John Wiley & Sons: New York, 1989.

MA061964Z